International Journal of Medical Arts

Volume 4, Issue 12, December 2022

https://ijma.journals.ekb.eg/

Print ISSN: 2636-4174

Online ISSN: 2682-3780

Available online at Journal Website
https://ijma.journals.ekb.eg/
Main Subject [Radiology]

Original Article

Role of Magnetic Resonance Imaging and Magnetic Resonance Spectroscopy in Differentiation Between Benign and Malignant Ovarian Lesions

Ahmed Zainhom Saleh Mohamed *[1], Mostafa M. Shakweer [1], Abdel-Naby Bioumy Mohamed [2]

[1] Department of Radiodiagnosis, Damietta Faculty of Medicine, Al-Azhar University, Damietta, Egypt
[2] Department of Radiodiagnosis, Faculty of Medicine, Al-Azhar University, Cairo, Egypt

Article information

Received: 11-09-2022

Accepted: 07-03-2023

DOI: 10.21608/IJMA.2023.162159.1509

*Corresponding author

Email: ahmedelnagar707@yahoo.com

Citation: Mohamed AZS, Shakweer MM, Mohamed AB. Role of Magnetic Resonance Imaging and Magnetic Resonance Spectroscopy in Differentiation Between Benign and Malignant Ovarian Lesions. IJMA 2022 December; 4 [12]: 2859-2875. doi: 10.21608/IJMA.2023.162159.1509.

ABSTRACT

Background: It is crucial to rule out any cancer in an ovarian mass. Following initial diagnosis, it is the most essential issue and has a significant impact on how the patient will be managed. Therefore, an accurate way to distinguish between a benign and malignant ovarian mass would allow for the best clinical evaluation and could perhaps lessen the number of unneeded laparotomies performed on benign lesions disease.

Aim of the Work: This work aims to investigate the quantitative and qualitative characteristics of proton MR spectroscopy [1 H-MRS] and to assess the effectiveness of 1H-MRS for distinguishing benign from malignant ovarian/adnexal tumors.

Patients and Methods: Forty patients with spotted adnexal/ovarian masses on primary pelvic ultrasound check referred to radio-diagnosis department at Al-Azhar university Hospital and National Cancer Institute. Twenty cases were benign, two were doubtful, and 18 were malignant.

Results: Standard MRI exhibited an accuracy of 70.6%, a sensitivity of 81.2%, a specificity of 61.1%, a positive predictive value of 65%, and a negative predictive value of 78.6%. We found that concurrent occurrence of both Cho and lactate peaks [the noise level was twice as loud as usual] increases the statistical accuracy in distinguishing benign from malignant ovarian masses from 85.3% with Choline alone and from 50 % with Lactate alone, to 93 % if both of them are found together. In combination of conventional MRI and proton MRS, we found increasing whole diagnostic accuracy of MRI in description of ovarian neoplasms, with sensitivity 96.5%, specificity 92.7%, positive predictive value 90.5%, negative predictive value 89% and accuracy 90.6%.

Conclusion: In vivo H^1 MRS is a non-invasive MR method that has creditable advantage in diagnosis of ovarian lesions with high specificity and positive predictive value. Combined analysis of conventional MRI and MR spectroscopy can achieve excellent results.

Keywords: Ovary; Magnetic Resonance; Imaging; Spectroscopy; Choline; Lactate.

INTRODUCTION

Adnexal masses are quite common and may be found in females of all ages, fetuses to the elderly [1]. A significant portion of these masses are the ovarian tumors which are classified into benign, borderline and malignant according to pathological characteristics [2].

Most importantly, any cancer in the pelvic mass must be ruled out. It is the first important step following the discovery of a mass and has a significant impact on the patient's care. Knowing the type of tumor before surgical intervention in a young lady is especially crucial [1]. So, A consistent way to distinguish between benign and malignant adnexal masses should allow for the best preoperative evaluation and maybe lessen the need for unneeded laparotomies for benign conditions [3].

Due to its outstanding tissue categorization and multi-planar imaging abilities, MRI can help with the accurate detection of benign disorders affecting the female pelvis [4]. Also, when it comes to the diagnosis, treatment, and follow-up of ovarian tumors, MRI is a useful instrument that can be utilized to distinguish benign from malignant or borderline from blatantly malignant ovarian tumors [2].

Despite the fact that MRI plays an important role in the discovery, deciding the source and expansion, and categorization of adnexal masses, there are considerable overlaps between benign and malignant tumors due to the various histologic categories and resultantly complex morphologic characteristics [5].

Functional MRI techniques referring to dynamic contrast-enhanced MRI [DCEMRI], diffusion-weighted imaging [DWI], intrinsic susceptibility- weighted [SWI] or blood oxygen level–dependent [BOLD] MRI; proton MR spectroscopy [MRS] are becoming established in the evaluation of gynecologic malignancies [6]. By monitoring the concentrations of proton-containing chemicals in tissues, proton MR spectroscopy [1H-MRS] is a non-invasive functional in vivo imaging technology that may study the biochemical processes [5].

THE AIM OF THE WORK

This work aims to investigate the quantitative and qualitative characteristics of proton MR spectroscopy and to assess 1H-effectiveness MRS's in separating benign from malignant ovarian/adnexal lesions.

PATIENTS AND METHODS

Study population: A prospective study included 40 patients with ovarian neoplasms as proposed by primary pelvic ultrasound testing. They were referred to the radio-diagnosis department at New Damietta Al-Azhar university Hospital. Lower abdomen pain, a sensation of weightiness in the pelvis, pelvic-abdominal swelling, losing weight, unusual lower back pain, vaginal bleeding, menstrual abnormalities, or urinary symptoms were among the symptoms of the patients who were included in the study.

Inclusion criteria: Ovarian and adnexal masses with the following characteristics: Purely cystic [greater than 5 cm] or solid masses, complicated cystic masses, and complex solid masses.

Exclusion criteria

1. Functional cysts.
2. Adnexal masses with pathology evidence that they are not of ovarian origin.
3. Pregnant patients.
4. Patients with elevated renal function tests.
5. Contraindications to MRI: cardiovascular pacemakers, cochlear implantation or other metal prostheses which impact the testing.

Pelvic MRI examination

Equipment: 1.5 T superconductive magnet device [Achieva, Philips Medical System, Best, Netherlands, Release 2.6, and Level 3], with multichannel phased-array coil [16 channels].

Technique:

A. Conventional MRI

1. **Survey [Field Echo],** Reffscan for the parallel imaging application.
2. **T1W series:** Axial TSE T1-weighted images without and with fat saturation
3. **T2w series:** Axial, coronal and sagittal TSE T2-weighted images.

B. Diffusion-weighted sequence: Diffusion-weighted MRI was obtained in the axial plane prior to administration of contrast medium using fat suppression in STIR–echo planar imaging sequence without breath holding with b values of 0 and 1000. Motion-probing gradient pulses were placed in the three orthogonal Z, Y, and X planes. Then, using equivalent imaging and free breathing, we produced axial half-Fourier single shot turbo spin echo fast spin echo [FSE] images as references. To confirm the lesion borders and prevent areas of obvious necrosis, ADC values were computed, and the TSE with parallel imaging at the same level—with or without the enhancedT1-weighted MR images—was referred to.

C. Dynamic contrast enhanced MRI: Using 3d FFE-T1 axial sequences, with adipose signal suppression [THRIVE], and multiplanar reformatted images. Scanning were acquired after bolus intravenous injection of paramagnetic Gd-DPTA contrast media [Magnevist] using a power injector at flow velocity of 2 ml/s and dose of 0.1 mMol/kgBW. Dynamic contrast enhanced series were obtained in seven acquisitions of one pre and six post contrast with 40 sec. interval time.

D. Proton MRI spectroscopy: We used multi-voxel spectroscopy [MVS] following recognition of lesions on T1-weighted and T2-weighted imaging. In case of large masses [> 4 cm] with homogenous components [i.e. purely cystic or solid masses] we used also the single voxel spectroscopy [SVS]. The localization technique was the point resolved spectroscopy [PRESS]: long echo time [TE] of 136 milli seconds, repetition time [TR] of 2000 milliseconds and 192 signal averages. The region of interest [ROI] for MRS dimension was positioned at the center of the examined mass to prevent signals from peripheral tissues becoming contaminated. Spectral reconstruction was conducted using software offered at the workstation of the MR device. Spectroscopic assessment of masses included measuring the signals from Lactate [Lac, 1.31 ppm], Lipid [Lip, 1.33 ppm], creatine [Cr 3 ppm], choline-containing compounds [Cho, 3.23 ppm], and N-acetyl aspirate [NAA, 2 ppm]. By estimating the identified peaks, patient spectra were evaluated, and a qualitative evaluation was carried out. Concentrations of choline and creatine were automatically calculated and semi-quantitative assessment was performed to approach the integral ratios [Cho/Cr].

Histopathological correlation*:* Correlation between magnetic resonance spectroscopic readings and post-surgical histo-pathological sections was performed in all cases. Surgical pathological findings served as the reference standard for assessment of ovarian tumors. Pathologists were unaware about the radiological results.

Post processing technique: Conventional MRI and functional imaging data were sent to and studied on an Advantage Windows workstation.

Conventional MRI: We evaluated the following MRI parameters: the volume of the mass, the thickness of the wall and the septa, the tissue composition, the lack or existence of necrosis in solid lesions, and the signal intensities on T1-weighted [fat-suppressed & nonfat-suppressed] and T2-weighted sequences. The cystic portion was described as tissue that did not enhance after injection and had homogenous long T1 and T2 features or varied signal intensities on T1- or T2-weighted MR images.

DCE- MRI: Non quantitative interpretation of DCE-MR views was completed using the region-of-interest [ROI] method. The regular outermost myometrium was employed as the internal standard, and ROIs were created there and in solid tissue on unenhanced MR images. In certain cases, we used multiple ROI: when the tumor showed a thickened irregular septum, many papillary projections, or a heterogeneous solid part.

Proton MRS: Patients' spectra were analyzed qualitatively by observing the peaks and semi-quantitatively using the Cho/Cr integral ratio. We used a ROC curve to detect the best cut-off value for Cho/ Cr intact ratio in distinguishing benign from malignant ovarian tumors.

Statistical analysis: The statistical program SPSS [Statistical Package for the Social Sciences] version 23 was used to code and enter the data. For quantitative data, the mean, standard deviation, median, minimum, and maximum were used; for categorical data, frequency [count] and relative frequency [%] were used. Sensitivity, specificity, Positive Predictive Value [PPV], Negative Predictive Value [NPV], and diagnostic accuracy were examined to determine the validity of both

conventional and functional MRI [DWI, DCE, and H1 MRS] for the diagnosis of ovarian lesions. The optimal Choline/Creat ratio cutoff value for cancer detection was discovered using an area under curve analysis ROC curve.

RESULTS

Pathological studies revealed that serous cystadenoma was the most prevalent benign disease, while serous/mucinous cystadeno-carcinoma was the most prevalent ovarian cancer [table 1].

Signal intensity strength on the DW images was assessed into three grades: low, high and mixed. Consensus was reached regarding the signal strength for each lesion. Signal intensities of grades 2 and 3 on DW images were deemed aberrant and possibly cancerous.

In this study, 29 masses showed grade 2 and 3 signal intensity, 19 masses out of them were pathologically proved to be malignant [true positive], while 10 masses found to be of benign nature [false positive]. On the other hand, grade 1 presented in 11 ovarian masses that was considered benign, correct diagnosis was achieved in 10 [true negative], and the remaining one turned to be malignant on histopathology [false negative]. The DW-MRI signal intensity demonstrated sensitivity of 94%, specificity of 50%, positive predictive value of 62%, negative predictive value of 90%, and accuracy of 70.5% for the distinction of benign and malignant ovarian neoplasms. All of the tumors had ADC values, and both benign and malignant tumors' mean ADC values were examined. In spite of the overlay in ADC quantities between the benign and malignant groups, the mean ADC value in the malignant tumors [0.78 x 10^3 mm^2/sec.] was significantly lower than that in the benign tumors [1.32 x 10^3 mm^2/sec].

We considered ovarian masses presented with type 2 and type 3 curves as malignant while those with type 1 curves as benign. Based on this, we reported 22 masses as malignant, out of them 17 masses were proven on histopathology to be true malignant [true positive]. The other 18 masses were reported as benign, out of them 15 were true benign [true negative] Table 2.

Cho peak twofold higher than the average noise level was detected in 16/18 of malignant masses [88.8%]: 4 masses of papillary serous cystadenocarcinoma, 5 masses of mucinous cystadenocarcinoma, one mass of granulosa cell tumor, 2 masses of undifferentiated carcinoma and one mass for each of clear cell carcinoma, dysgerminoma and two Immature teratoma. For 20 benign masses included**,** only two benign masses [fibroma] showed Cho peak is two times louder than the background noise. We believed that the Cho peak, which was twice as loud as the background noise, was a sign that a tumour was malignant and that it could be distinguished between benign and malignant ovarian masses with a sensitivity of 76%, specificity of 93.5%, positive predictive value of 91.6%, negative predictive value of 82%, and accuracy of 85.7%.

In 12 invasive malignant tumours, the Cr peak was found. All benign [n = 20] and borderline malignant [n = 2] tumours had low Cr signals Table 3.

The ROC curve analysis of choline-to-creatine ratio produced an AUC of 0.919 and a level of 1.7 for diagnosing malignant ovarian tumors with sensitivity of 80.5%, Specificity of 92.7 %, Positive predictive value of 93 %, Negative predictive value of 81.5 %, and Accuracy: 87% Table 4.

Lactate peak was detected in 14 /18 of malignant masses [77.7%] 3 out of 4 cases of papillary serous cystadenocarcinoma, 5 masses of mucinous cystadeno-carcinoma, 2 out of 3 masses of granulosa cell tumor, one mass of clear cell carcinoma, one mass of dysgerminoma, one out of two masses of undifferentiated carcinoma and one mass of borderline mucinous cystic tumor. Lactate peak was detected in 10 cases [50%]: hemorrhagic cysts [3 cases], tubo-ovarian abscesses [3 cases], endometrioma [2 cases], serous cystadenoma [2 out of 4 cases] and fibro-thecoma [1 case]. No lactate peak was detected in: three masses of mucinous cystadenomas, and two masses of fibroma and another two mature cystic teratoma.

Lipid peak was detected in 16 /18 of malignant cases [88.8%] [3 out of 4 cases of papillary serous cystadenocarcinoma], [4 out of 5 masses of mucinous cystadeno-carcinoma], [3 masses of granulosa cell tumor], [one mass of dysgerminoma], [two masses of immature teratoma], [one out of two masses of undifferentiated carcinoma].

NAA peak was detected in 8/20 benign cases: serous cystadenoma [4 cases], fibroma [2 cases] and mature cystic teratoma [2 cases]. NAA peak was noted in mucinous cystadenoma [3 cases], Tubo-ovarian abscess [1 out of 3 cases], hemorrhagic cyst [2 out of 3 cases] and fibro-thecoma [1 case].

The statistical indices for the combined analysis conventional MRI and proton MRS in characterization and differentiation ovarian neoplasms are: Sensitivity: 96.5%, Specificity: 92.7%, Positive predictive value: 90.5%, Negative predictive value: 89%, Accuracy: 90.6%.

Table [1]: Histopathological results of the 40 masses in this study

		Count	%
Benign	Hemorrhagic Corpus Lutiem cyst	3	15%
	Tubo-Ovarian Abscess	3	15%
	Endometriotic Cyst	2	10%
	Serous Cystadenoma	4	20%
	Mucinous Cystadenoma	3	15%
	Fibroma	2	10%
	Fibro-thecoma	1	5%
	Mature Cystic teratoma	2	10%
Malignant	Serous Cystadeno carcinoma	4	22.2%
	Mucinous Cystadeno carcinoma	5	27.7%
	Clear cell adenocarcinoma	1	5.5%
	Granulosa Cell tunor	3	16.6%
	Undifferentiated carcinoma	2	11.1%
	Immature teratoma	2	11.1%
	Dysgerminoma	1	5.5%
Borderline	Borderline serous cystic tumor [low malignant potential]	1	50.0%
	Borderline mucinous cystic tumor	1	50.0%

Table [2]: Shows lesion dynamic enhancement pattern curves in this study

		DCE-MRI Type of Curve		
		Type 1 curve=Gradual increase without shoulder	**Type 2 curve=Initial rise followed by plateau**	**Type 3 curve= Steeper rise than myometrium**
		Count	**Count**	**Count**
Benign	Hemorrhagic Corpus Lutiem Cyst	2	1	0
	Tubo-Ovarian Abscess	2	1	0
	Endometriotic Cyst	0	2	0
	Serous Cystadenoma	4	0	0
	Mucinous Cystadenoma	3	0	0
	Fibroma	2	0	0
	Fibro-Thecoma	0	1	0
	Mature Cystic Teratoma	2	0	0
Malignant	Serous Cystadeno Carcinoma	0	3	1
	Mucinous Cystadeno Carcinoma	0	4	1
	Clear cell Adenocarcinoma	0	0	1
	Granulosa Cell tumor	0	3	0
	Undifferentiated Carcinoma	0	1	1
	Immature Teratoma	0	0	2
	Dysgerminoma	1	0	0
Borderline	Borderline Serous Cystic Tumor	1	0	0
	Borderline Mucinous Cystic Tumor	1	0	0

Table [3]: Shows mean Cho/Cr Ratio values in patients in this study

		Mean Choline/Creat
		Mean
Benign	Hemorrhagic Corpus Lutein Cyst	1.09
	Tubal/Ovarian Abscess	1.29
	Endometrial Cyst	1.19
	Benign serous Cysta-denoma	0.75
	Benign Mucinous Cystadenoma	0.75
	Fibroma	3.79
	Fibro-Thecoma	1.08
	Mature Cystic Teratoma	.
Malignant	Serous Cystadeno Carcinoma	3.30
	Mucinous Cystadeno Carcinoma	3.19
	Clear cell adenocarcinoma	2.89
	Granulosa Cell Tumor	2.19
	Undifferentiated carcinoma	2.92
	Immature Teratoma	1.89
	Dysgerminoma	4.48
Borderline	Borderline serous cystic tumor	1.28
	Borderline mucinous cystic tumor	2.28

Table [4]: ROC curve of cho/cr ratio in the diagnosis of ovarian malignant masses

AUC	P value	95% CI		Cutoff value	Sensitivity	specificity	PPV	NPV	Accuracy
		Lower	Upper						
0.920	**<0.001**	.802	1.035	1.7	80.5%	92.7%	93	81.5%	87%

Table [5]: Diagnostic performance of various spectral metabolites in the detection of malignant ovarian masses

Metabolites	Sensitivity	Specificity	Accuracy	PPV	NPV
Choline	76	93.5	85.7	91.6	82
Choline/creatine [1.7]	80.5	92.7	87	93	81.5
Lactate	69.1	33.2	52	48	53.6
Choline + lactate	93.8	90	93	92.3	85
Lipid	73	60	65	60	70
N-acetyle aspartate	44	30	37	39	34
Convetional MRI + MRS [all metabolites]	96.5	92.7	90.6	90.5	89

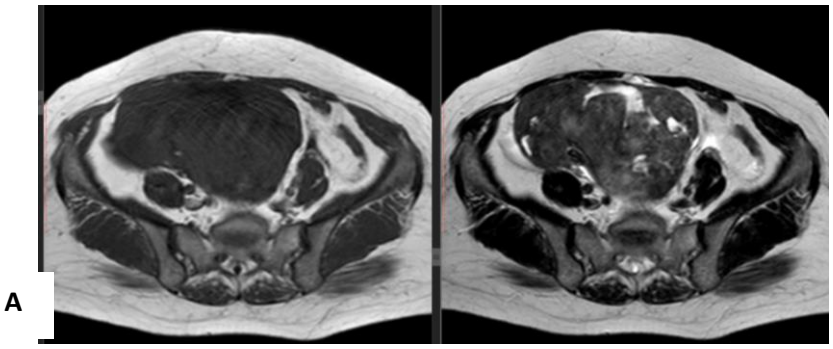

A

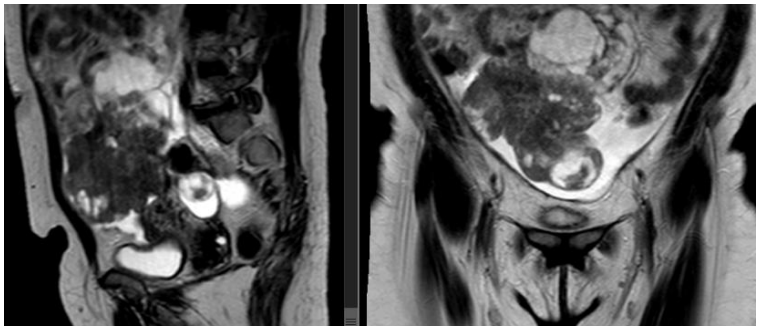

B

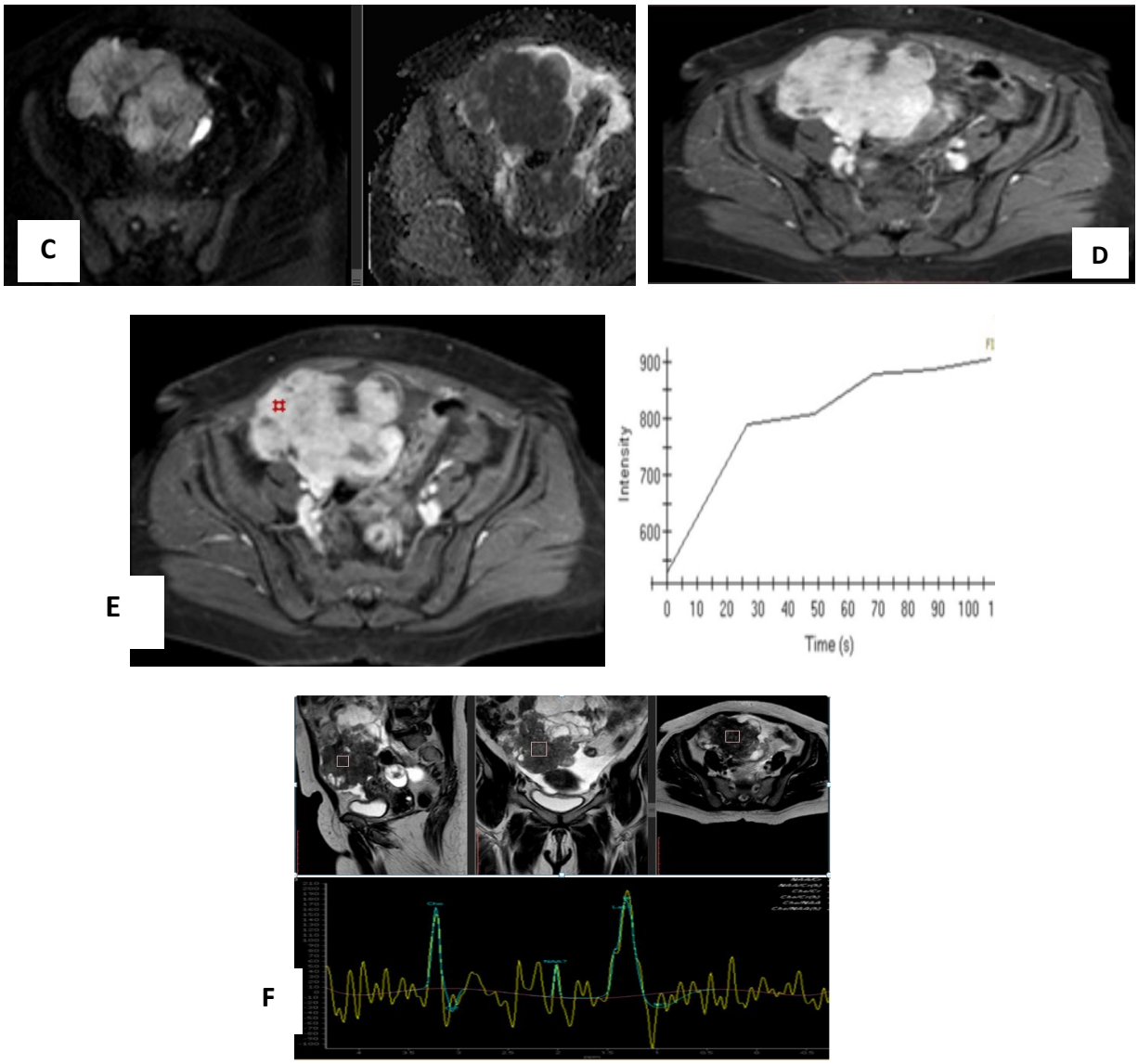

Figure [1]: A 26 -years-old female patient, presented with pelvic pain and vaginal bleeding. US Duplex study showed pelvi-abdominal complex cystic mass with thick vascular septae and solid components**; [A]:** Axial T1 & T2-weighted image through the pelvis showing large pelvi- abdominal predominantly cytstic mass with both septations and solid components**; [B]:** coronal T1-postcontrast and coronal T2-weighted image through the pelvis showing the mass extremely heterogeneous being partially solid partially cystic, with enhancement of the solid component. Ascites is also noted**; [C]:** Axial diffusion-weighted imaging [DWI] and ADC reveals restricted diffusion of tumoral solid parts with mean ADC value = 0.9 x10-3mm2/s**; [D]:** Post contrast Axial T1-weighted image with fat saturation through the mass reveals avid enhancement of solid components**; [E]:** DCE-MRI, the solid part of the mass is enhanced with a moderate initial rise relative to that of myometrium followed by a plateau "curve type 2."**; [F]:** Single voxel proton MRS showing sharp choline peak, Cho/Cr: 4.5. Also, sharp lactate/lipids peaks are also noted. NAA signal is detected. **Final diagnosis:** Right ovarian dysgerminoma

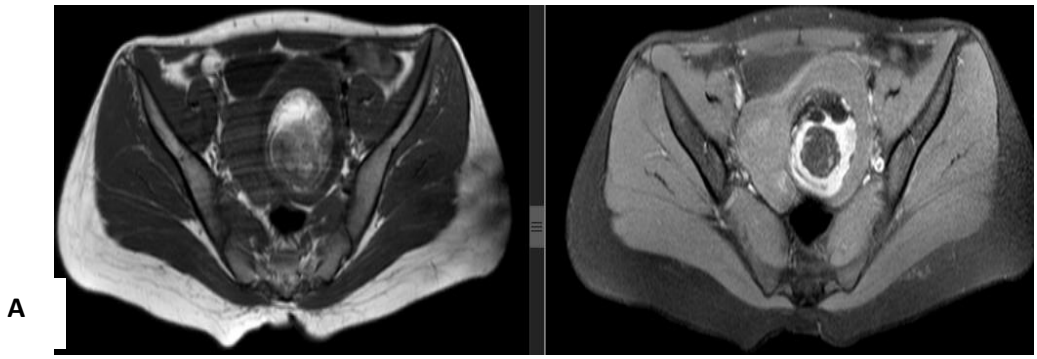

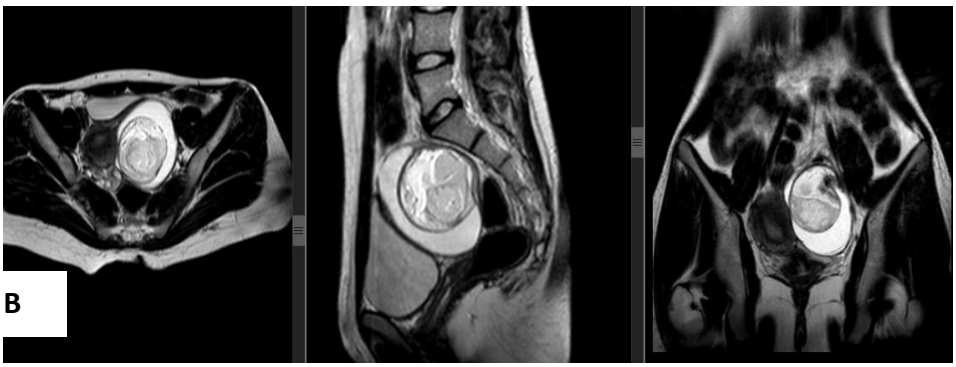

B

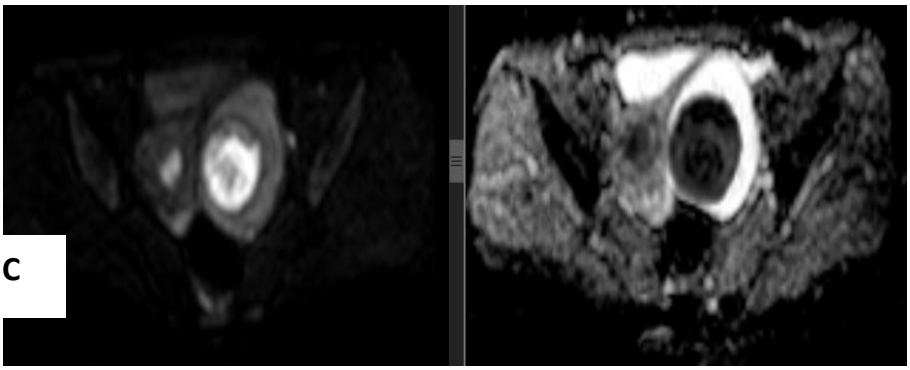

C

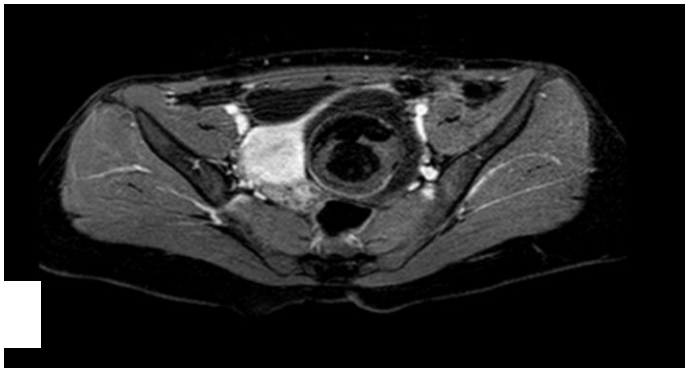

D

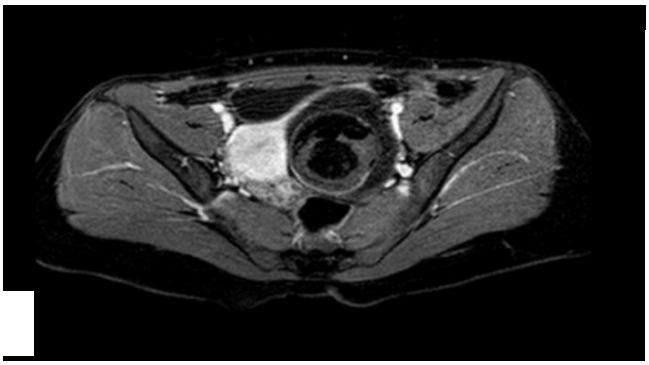

E

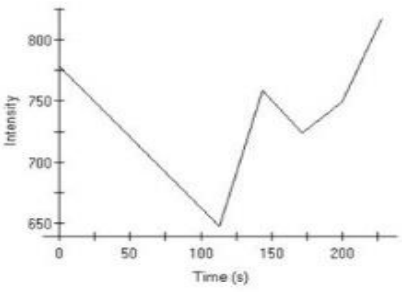

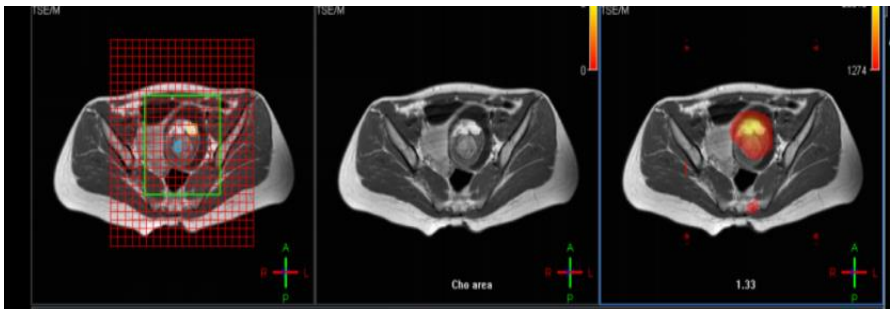

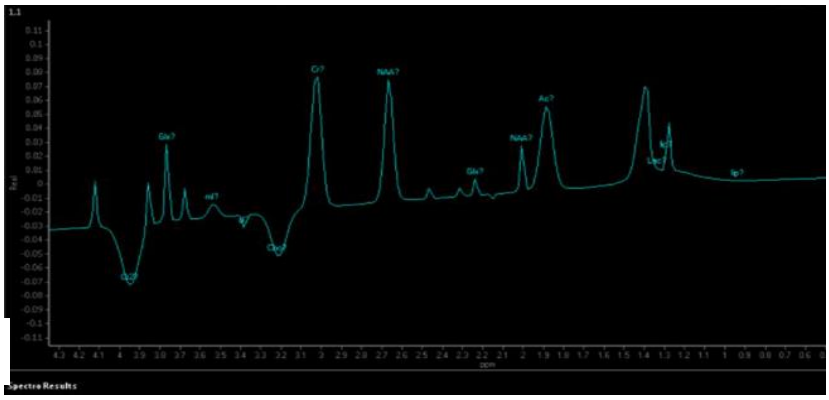

F

Figure [2]: A 21 -years-old female patient, presented with lower abdominal pain, US showed left adnexal complex cystic mass**; [A]:** Axial T1-weighted image & T1WI with Fat saturation through the pelvis showing left adnexal isointense mass with focal peripheral hyperintensity that shows signal drop in the fat saturation sequence.[m: mass]**; [B]:** Axial, sagittal and coronal T2-weighted image through the pelvis showing complex partially solid partially cystic mass with small hypointense spot likely to be calcification [m: mass, u:uterus, r:rectum, ub:urinary bladder]**; [C]:** Axial diffusion-weighted imaging [DWI] and ADC mapping reveals that part of the mass has moderate high signal intensity on DWIs with mean apparent diffusion coefficient [ADC] = 0.9 x10-3mm2/s**; [D]:** Post contrast Axial T1-weighted image with fat saturation through the mass reveals no significant post contrast enhancement**; [E]:** DCE-MRI, the solid part of the mass is not enhancing with bizarre shaped curve**; [F]:** Proton MRS showing sharp NAA, lactate/ lipids peaks and smaller lipid peak .Cho/Cr ratio: 0.3**; Final diagnosis:** Left ovarian mature cystic teratoma.

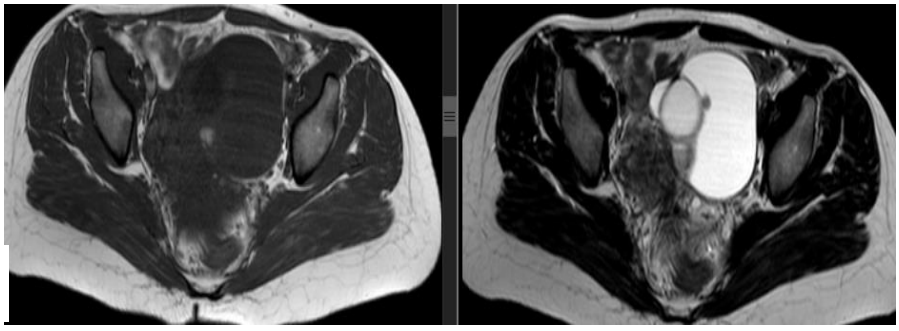

A

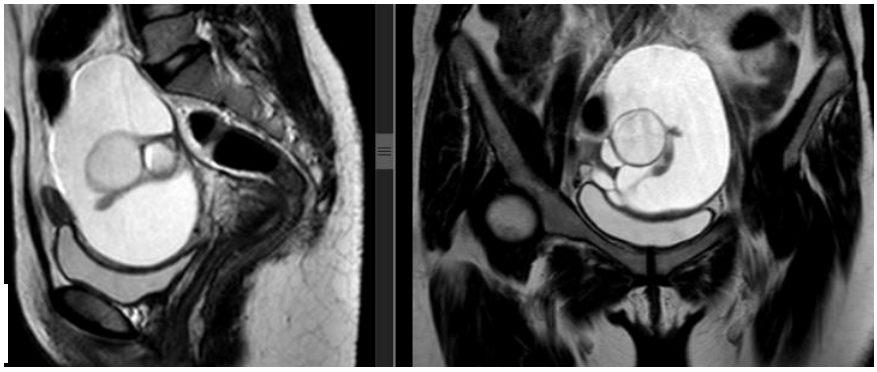

B

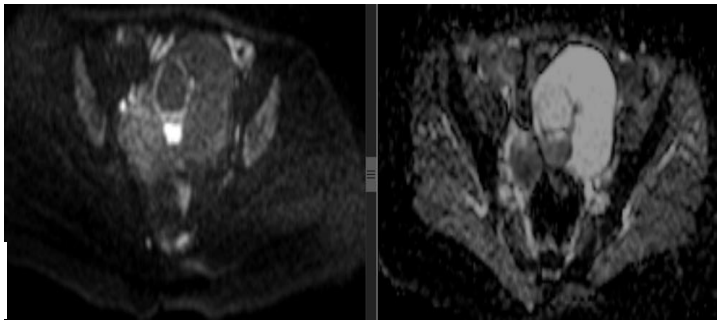

C

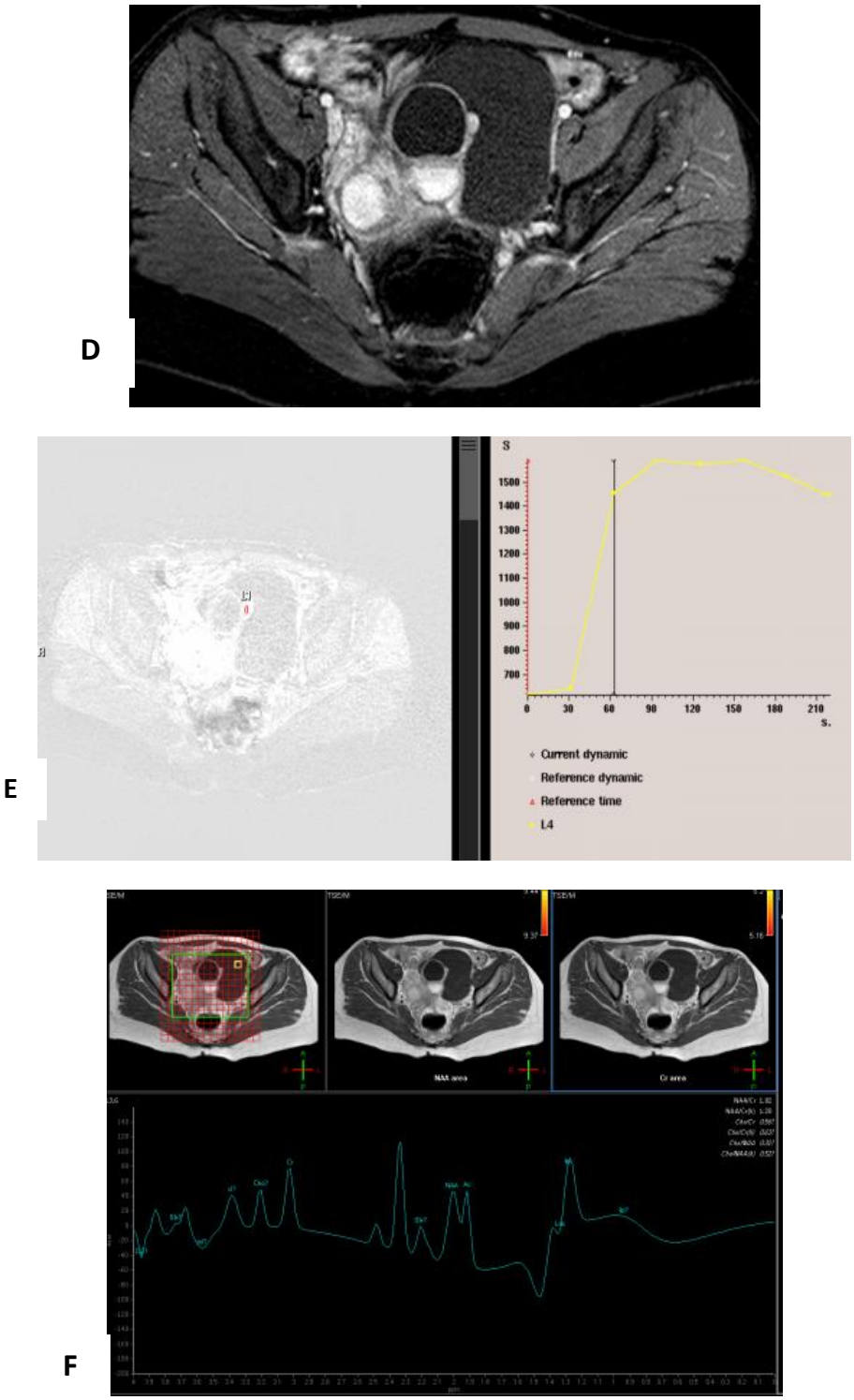

Figure [3]: A 28-year-old female patient presented with swelling and urinary incontinence. Preliminary US was done and revealed left ovarian complex cystic lesion**; [A]:** Axial T1 & T2 -weighted images showing left adnexal multilocular cystic lesion that shows thick internal septations reaching 1cm in thickness. It elicits low T1 and high T2 signals interpersonal hemorrhage of high T1 and T2 signal intensity**; [B]:** Sagittal and coronal T2-weighted image through the pelvis showing the mass is of multilocular cystic lesion that shows thick internal septations reaching 1cm in thickness of high T2 signal**; [C]:** Axial diffusion-weighted imaging [DWI] and ADC mapping, reveals diffusion restriction of the internal septations. ADC value measures $1.1x10^{-3}mm^2/S$**; [D]:** Post contrast axial T1-weighted image with fat saturation, through the mass reveals heterogeneously enhancing nature of the mass**; [E]:** DCE-MRI, DCE shows the thick septations is of type II curve: initial rapid rise followed by a plateau with delayed washout**; [F]:** The spectrum shows a sharp choline peak of its solid and fluid components, lipid/lactate peak, and NAA peak. Cho/Cr: 1.3**; [Final diagnosis]:** Left ovarian borderline mucinous cystadenoma

A

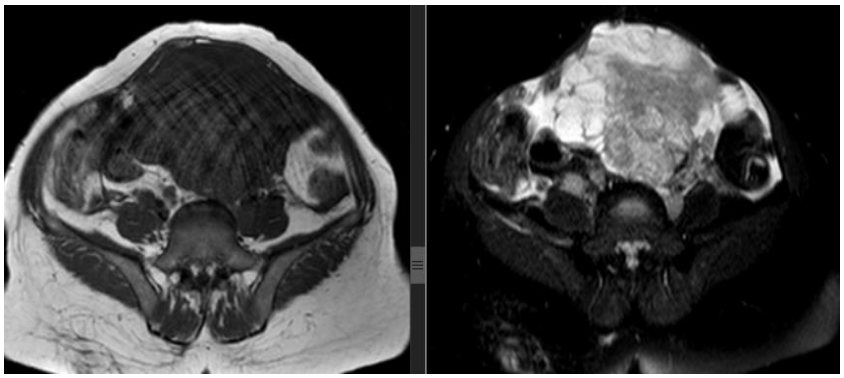

B

C

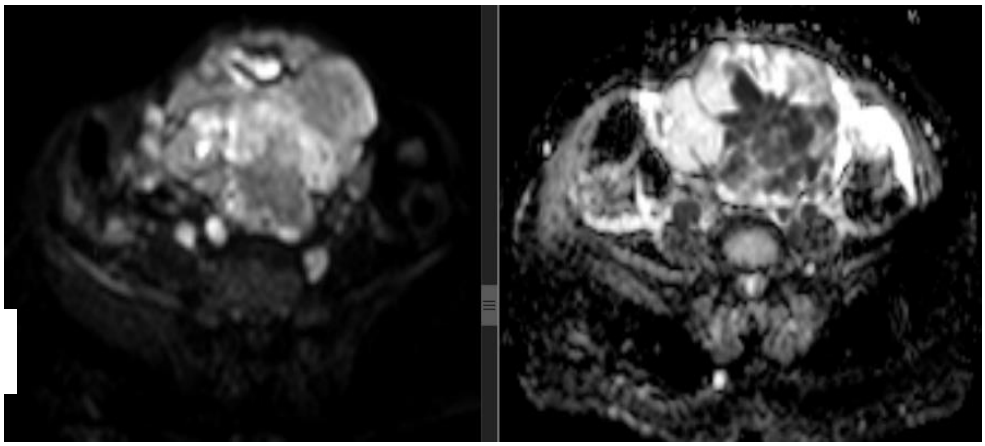

D

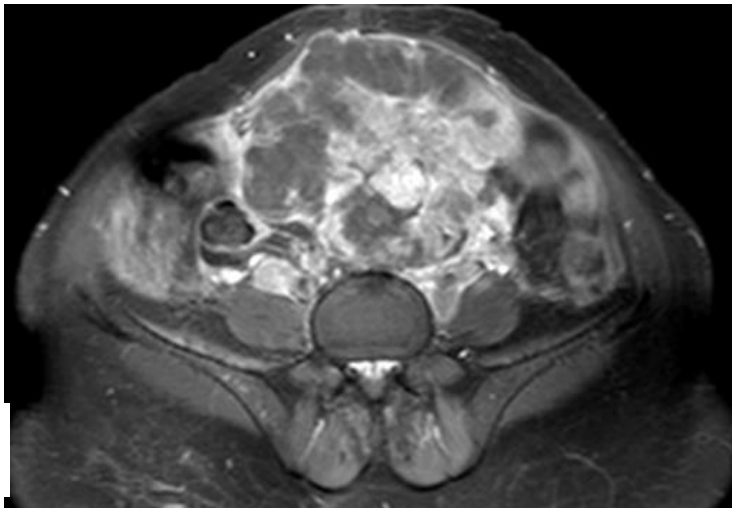

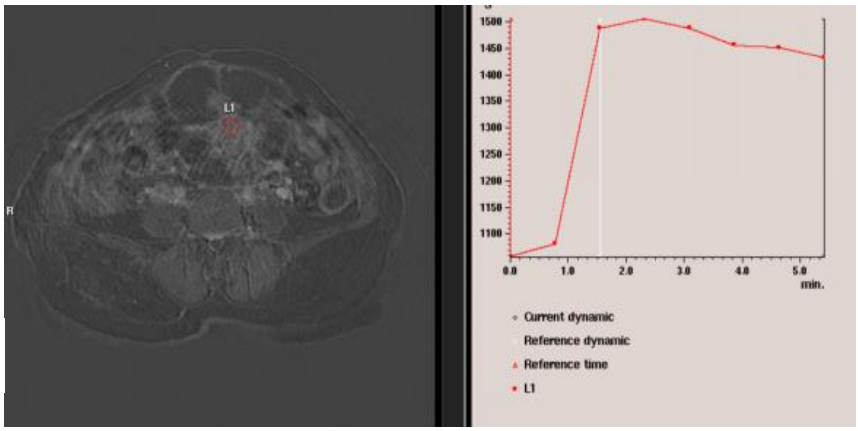

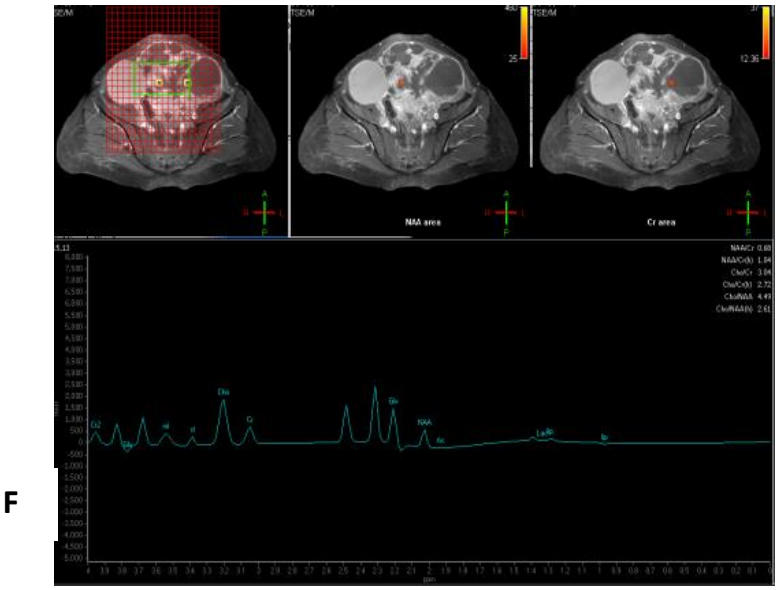

Figure [4]: A 52 -years-old female patient, presented with pelvic pain and swelling, US showed left pelvic complex cystic mass with solid components**; [A]:** Axial T2 & T1 -weighted images through the pelvis showing left adnexal large heterogeneous predominantly cystic mass**; [B]:** Coronal T1 and T2-weighted image through the pelvis**; [C]:** Axial diffusion-weighted imaging [DWI] and ADC reveals that the solid part of the mass has a restricted diffusion with mean ADC value=0.9 x10-3mm2/s**; [D]:** Post contrast Axial & sagittal T1-weighted image with fat saturation through the mass showing heterogeneous pattern of enhancement with strongly enhancing thick wall and solid portions**; [E]:** DCE-MRI, the solid part of the mass is enhanced with initial rise followed by plateau "curve type 2."**; [F]:** Single voxel proton MRS showing small choline peak, Cho/Cr ratio: 2.2, also lactate/lipid signal is noted**; Final diagnosis:** Left ovarian mucinous cyst adenocarcinoma

DISCUSSION

Imaging plays a crucial role in management preparation for many ovarian masses that are inadvertently discovered by distinguishing benign from borderline or aggressive malignant tumors as management planning differs for. Surgery might not be necessary if a lesion is correctly classified as benign [7].

This is essential because borderline malignant tumors typically affect young women who want to retain their ability to have children and are linked to minimal recurrence and high overall survival rates, necessitating conservative laparoscopic surgery [8].

In this study, we assessed the role of MR spectroscopy as a non-invasive functional MR imaging sequence in the distinction between benign and malignant ovarian masses. In our evaluation we first analyzed the morphology and internal components of the included ovarian tumors. The typical histologic form in the examined malignant lesions was the complex solid masses, whether with septae and/ or solid nodules. This is found in 12 out of 18 tumors, about 66.6 %, illustrated in case [1, 4]. Purely cystic design was not seen among any of the cancerous ovarian tumours that were included.

These results are in agreement with studies of **Bazot *et al.*** [9], who performed MRI in 136

women with sonographically indeterminate adnexal masses [99 benign, 23 borderline and 46 invasive]. They reported that most of malignant tumors were cystic with both solid nodule and septa. Similar results were also encountered in works of **Moyle *et al.*** [10] and **Foti *et al.*** [11], investigated 65 patients with ovarian tumors, reported that most of the benign tumors were purely solid or cyst with thin septa, yet cystic masses combined with solid nodules was the most common type in the malignant group. **Lam *et al.*** [12] prospectively studied 72 women with clinically suspected adnexal masses. They suggested malignancy whenever there were large masses and solid-cystic lesions with nodules.

Considering the signal intensity, the majority of benign and malignant tumors displayed low or similar intensity on T1WI with heterogeneous hyper intensity on T2W as demonstrated in illustrative case [1]. These findings were found in 11 out of 20 benign tumors, about [55%] and in 11 out of 18 malignant tumors, about [61.1 %]. However, between benign and malignant tumors, there were no appreciable variations in the MRI signals.

Some studies revealed variations between MRI signals among benign and cancerous lesions as in **Zhao *et al.*** [2] who studied 26 benign mucinous cystadenomas and 24 borderline mucinous cystadenomas of the ovary. They stated that the ovarian borderline mucinous cystadenoma can be identified using MRI. Benign mucinous cystadenoma had the most significant feature of high signal intensity on T1WI and low signal intensity on T2WI of the intracystic content.

Bazot *et al.* [9] mentioned that; on T2-weighted MRI, low solid-tissue signal intensity was helpful in separating benign from aggressive ovarian cancers

Low solid-tissue signal intensity on T2-weighted MRI is suggestive of benignity, according to **Sohaib *et al.*** [13], who prospectively performed MR imaging in 104 patients with clinically or sonographically-diagnosed complicated adnexal masses

In our investigation, conventional MRI demonstrated sensitivity of 81.2%, specificity of 61.1%, positive predictive value of 65%, negative predictive value of 78.6%, and accuracy of 70.6% for differentiating benign and malignant ovarian neoplasms. Our outcomes were comparable to **Foti *et al.*** [11] and **Bazot *et al.*** [9]**.** However other studies had higher sensitivity, specificity, accuracy, or positive predictive values than we had, where **Lam *et al.*** [12], obtained MRI sensitivity, specificity and accuracy of 96.6%, 83.7% and 88.9%, respectively.

According to **Adusumilli *et al.*** [14], MRI's sensitivity for accurately identifying a malignant lesion was 100% and its specificity for accurately diagnosing a benign lesion was 94%.

The discrepancy between their results and ours was likely attributed to the lower number of malignant masses they included in their study.

Tumor vascularity, tissue microarchitecture, hypoxic status, and metabolic profile can all be examined using parameters generated from functional MRI techniques. These characteristics can be used for tumor characterization, staging, or as predictive or response biomarkers of prognosis and response [6].

We defined suggested lesions with persistent bright signal intensity as malignant ovarian lesions. On DW-MRI signal intensity, 29 masses were reported as malignant [grade 2 and 3 signal intensity], out of them 19 were true positive [62.5%]. On the other hand, 11 masses were reported as benign lesions [grade1 signal intensity], out of them 10 [90.9%] true negative. Most of the malignant tumors [94.4%, n=17/18] gave high/mixed signals as demonstrated in illustrative case [1, 4], while most of the benign tumors [15/20] about [75%] gave low signals as demonstrated in illustrative case [2]. DW-MRI signal intensity showed a sensitivity of 94%, specificity of 50%, positive predictive value of 62%, negative predictive value of 90%, and accuracy of 70.5 for differentiating benign and malignant ovarian neoplasms.

Our results were in agreement with **Foti *et al.*** [11], who investigated 65 patients with ovarian tumors, reporting that there was a significant difference between non-malignant and malignant lesions in their series as most of the malignant tumors [27/42] about 84% had high signal, and this was obvious in most malignant lesions.

Messina *et al.* [15] studied 49 surgically confirmed ovarian cancers [39 malignant/borderline malignant and 10 benign]. They discovered that only 3 of the 10 benign tumours had homogeneous or heterogeneous high intensity on DWI in their solid regions

Bakir *et al.* [16] performed, DWI for 37 solid adnexal masses [22 malignant and 15 benign neoplasms]. They observed on DWI, high signal intensity was more often in malignant than in benign lesions.

According to **Kim *et al.*** [17]*'s* research, aberrant DWI signal intensity cannot be used to distinguish between benign and malignant ovarian tumors. This disappointing outcome is primarily the result of benign tumors with abnormally high levels of intensity, particularly mature cystic teratomas and endometriomas.

For differentiation of benign and malignant ovarian neoplasms, ADC values reached correct diagnosis in 63.5% of the malignant and 90% of the benign ovarian masses. The statistical indices were: sensitivity 93.8 %, specificity 50 %, positive predictive value 62.5 %, negative predictive value 90 % and accuracy 70.6 %.

A total of 127 individuals with 131 pelvic masses were enrolled by **Li *et al.*** [18]. They claimed that compared to benign tumours, malignant ovarian surface epithelial tumours had mean ADC values that were considerably lower.

Koc *et al.* [19]**,** studied 66 lesions of gynecological diseases were in their study. With a sensitivity of 83% and a specificity of 70%, they reported that the mean ADC values of malignant masses were considerably lower than those of benign lesions for all P values [$P < 0.005$]. However, our results were different in opinion from other studies, where **Bakir *et al.*** [16]**,** observed that the ADC values of the malignant and benign lesions in either the adnexal or the ovarian lesions did not significantly differ. Also, **Messina *et al.*** [15]**,** who found ADC values were insufficient to distinguish between benign and malignant adnexal masses.

We considered masses that showed type 2 and type 3 curve patterns as malignant lesions which were demonstrated in illustrative case [1-4].

DCE time intensity curves demonstrated sensitivity of 75%, specificity of 72.5, positive predictive value of 70.5, negative predictive value of 76.5, and accuracy of 73.5 in identifying malignant from benign ovarian tumors.

Our results were comparable with some studies where, **Wakefield *et al.*** [6] found that non-quantitative DCE-MRI showed 77% sensitivity and 75% specificity in the distinguishing malignant from benign ovarian tumors. **Messina *et al.*** [15]**,** supported the addition of perfusion weighted [PW] to diffusion weighted [DW] images which led to a correct change in the diagnosis in 19%-24% in their study.

In this study, MRS was performed in all cases using multi-voxel and/or single voxel spectroscopy using PRESS localization technique. The spectra of the patients were analysed subjectively by looking at the peaks of lipid, creatine, lactate, and N-acetyl aspirate, as well as quantitatively by using the Cho/Cr integral ratio. In our study, a Cho peak was found in 16 out of 18 of malignant cases as demonstrated in illustrative case [1] while it is found in only 1 out of 20 benign cases as demonstrated in illustrative case [3]. We considered that choline peaks an indicator that a tumor was malignant in nature.

Iorio *et al.* [20] analyzed the different moieties that make up the total choline resonance and discovered that cancerous ovarian cells had significantly higher amounts of phosphocholine and total choline than healthy ovarian cells did.

Identification of a choline peak revealed 89% sensitivity and 84% specificity in differentiating malignant from benign disease in 23 ovarian tumors, according to **Esseridou *et al.*** [21].

Vang *et al.* [22] analyzed the spectra from 25 patients with adnexal lesions. They stated that only benign lesion did not show a choline peak, with except for mucinous cyst-adenoma, However, they explained that the choline peak appreciable in mucinous cystadenoma was considerably lower compared to the one evaluated in malignant lesions.

Because in vivo 1H-MRS has a lesser spectrum resolution than in vitro 1H-MRS,

investigations employ the ratio of peak integral to describe, quantify, and contrast metabolic alterations among various malignancies [5].

We considered Cho/Cr integral ratio of > 1.7 as a reference that a tumor was malignant in nature. 18 masses had been reported on MRS curves as malignant lesions, out of them 15 [94.4%] were true positive as demonstrated in illustrative case [4]. Also, 20 masses reported as benign with 17 [85%] true negatives as demonstrated at illustrative case [2]. Two masses showed incorrect category; one was false positive as demonstrated in illustrative case [3] and another one was false negative.

Our results were in agreement with **Li *et al.*** [23] who discovered that a choline peak-to-creatine ratio threshold of 2 may successfully distinguish between benign and malignant adnexal tumors and **El Sorogy *et al.*** [24] reported that malignant ovarian masses had a mean Cho/Cr ratio that was substantially greater than benign ovarian masses

Forstner *et al.* [25] used 3 Tesla MRI to perform MRS on ovarian masses. According to their findings, a tumor's choline/Cr integral ratio larger than 3 suggests that it is malignant, but a tumor's choline/Cr integral ratio less than 1.5 was shown to be benign.

In our study, a lactate peak was detected in 14 out of 18 of malignant cases as demonstrated in illustrative case [1], however it is also found in 12 out of 20 benign cases as demonstrated in illustrative case [2]. We considered that lactate peak an indicator that a tumor was malignant in nature. Based on that, lactate peak demonstrated Sensitivity 69.1%, Specificity 33.2%, Positive predictive value 48%, Negative predictive value 53.6%, and Accuracy 52% in discriminating benign from malignant ovarian lesions. These results were matched with a study of **Ma *et al.*** [5]. On the contrary, **Kang *et al.*** [26] found lactate signal was characteristically obtained not just in all malignant cancers but in certain benign ones as well. However, compared to benign tumors, the lactate signals from malignant tumors tended to produce greater peaks.

We made an effort to investigate the statistical importance of the concurrent existence of the Cho and lactate peaks in distinguishing between benign and malignant ovarian tumors. The accuracy increased from 85.3% with choline alone and from 50% with lactate alone to 93% when the two were combined, which is an interesting finding.

Our data has been in concurrence with **Vargas *et al.*** [27], who concluded that the simultaneous observation of a choline peak together with a lactate peak is a stronger malignancy predictor rather than the presence of a choline, or lactate peak alone.

Also, compared to benign cysts, ovarian neoplasms with moderate to poor histological differentiation have been observed to have higher intracellular lactate levels and total choline compounds, according to **Abramov *et al.*** [28].

Different types of malignant tumors may contain lipid. Malignant ovarian tumors and benign teratomas both exhibited a strong lipid peak at 1.3 ppm, according to **Cho *et al.*** [29], whereas normal epithelial ovarian tumours did not.

We detected lipid peak in 16 /18 of malignant masses as demonstrated in illustrative case [1] but also in 12/20 benign masses as demonstrated in illustrative case [2]. In the present study; all cases of teratomas and abscesses showed lipid peak at 1.3 ppm as demonstrated in illustrative cases [2].

Spectroscopy investigation of adult cystic teratomas reveals the presence of NAA metabolites, indicating the existence of neural element [ectodermal tissue]. Although lacking neural tissue, it is also present in simple follicular cysts, cyst fluid from serous cystadenomas, and both solid and cystic portions of mucinous cystadenoma [26].

That was going with the results of this study where NAA was detected in a case of serous cystadenocarcinoma as demonstrated in illustrative case [4] and a case of dysgerminoma in illustrative case [1].

However other studies showed different opinion where **Takeuchi *et al.*** [30] stated found when combined with choline, N-acetyl resonances at 2.0 ppm enhanced the possibility of ovarian metastases with 89% sensitivity and 86% specificity in the detection of mucinous components.

In our study, we found that several factors may restrict the use of 1H-MRS in the

evaluation and follow-up of malignant illness; 1] At field strength of 1.5 T, chemicals apart from Cho that are suggestive of cancer is limited are more difficult to detect because of their significantly lower quantities [0.01 mol/L for Cho vs. 0.00001 mol/L or lower for various tumour related chemicals], 2] the variety of samples and the intricate histopathologic characteristics of tumors, 3] Lactate signal was found to be confused by intersecting with extra powerful lipid resonances, 4] No actual quantitative study was done; only the ratio of metabolites [Choline] to creatine was evaluated. In addition to making inter-patient comparisons easier, quantification also makes it possible to establish more objective detection criteria and conduct longitudinal research despite potential tumour size fluctuations. Although the creatine ratio approach takes into account some of these issues, it depends on quantifying a peak that is often smaller than choline and could hence amplify experimental mistakes, 5] Regarding adnexal masses, the usage of MRS was restrained to in vivo researches due to respiratory and bowel movements.

Finally, the combination of conventional MRI and proton MRS, as ovarian neoplasms were characterized, we saw an increase in the overall diagnostic accuracy of MRI, with sensitivity, specificity, positive predictive value, negative predictive value, accuracy, and accuracy ratios of 96.5%, 92.7%, 90.5%, and 90.6%, respectively

However, additional research comprising a large number of cases is necessary so as to establish indicators of in vivo MRS diagnosis of pelvic masses.

Disagreement of our results with certain studies could be attributed to: Different inclusion criteria, a] where we included only ovarian masses while other studies included all adnexal masses, whether ovarian or non-ovarian as seen in several studies [3, 8, 18], b] All ovarian lesions whether neoplastic or non-neoplastic were studied in our study, while other studies evaluated only ovarian epithelial tumors [2, 8], C] Different sample size: we evaluated 40 patients while other studies had different sample size as in studies of **Bazot *et al.*** [9] [n=136], **Lam *et al.*** [12] [n=72], **Zhao *et al.*** [2] [n=50], **Foti *et al.*** [11] [n=601] and **Kim *et al.*** [17] [n=123].

Conclusion: In vivo H^1 MRS is a noninvasive MR technique that has creditable advantage in diagnosis of ovarian masses with high specificity and positive predictive value. Combined analysis of conventional MRI and MR spectroscopy can achieve excellent results.

Conflict of Interest and Financial Disclosure: None.

REFERENCES

1. Dwivedi AN, Jain S, Shukla RC, Jain M, Srivastava A, Verma A. MRI is a state of art imaging modality in characterization of indeterminate adnexal masses. J Biomed Sci Engin. 2013;6:309-13.
2. Zhao SH, Qiang JW, Zhang GF, Wang SJ, Qiu HY, Wang L. MRI in differentiating ovarian borderline from benign mucinous cystadenoma: pathological correlation. J Magn Reson Imaging. 2014 Jan;39[1]:162-6. doi: 10.1002/jmri.24083.
3. Dogheim OY, Hamid AE, Barakat MS, Eid M, El-Sayed SM. Role of novel magnetic resonance imaging sequences in characterization of ovarian masses. Egyptian Radiol Nuclear Med. 2014 Mar 1;45[1]:237-51.
4. Masselli G, Gualdi G. MR imaging of the placenta: what a radiologist should know. Abdom Imaging. 2013 Jun;38[3]:573-87. doi: 10.1007/s00261-012-9929-8.
5. Ma FH, Qiang JW, Cai SQ, Zhao SH, Zhang GF, Rao YM. MR Spectroscopy for Differentiating Benign From Malignant Solid Adnexal Tumors. AJR Am J Roentgenol. 2015 Jun;204[6]:W724-30. doi: 10.2214/AJR.14.13391.
6. Wakefield JC, Downey K, Kyriazi S, deSouza NM. New MR techniques in gynecologic cancer. AJR Am J Roentgenol. 2013 Feb;200[2]:249-60. doi: 10.2214/AJR.12.8932.
7. Wasnik AP, Mazza MB, Liu PS. Normal and variant pelvic anatomy on MRI. Magn Reson Imaging Clin N Am. 2011 Aug;19[3]:547-66; viii. doi: 10.1016/j.mric.2011.05.001.
8. Thomassin-Naggara I, Balvay D, Aubert E, Daraï E, Rouzier R, Cuenod CA, Bazot M. Quantitative dynamic contrast-enhanced MR imaging analysis of complex adnexal masses: a preliminary study. Eur Radiol. 2012 Apr;22[4]:738-45. doi: 10.1007/s00330-011-2329-6.
9. Bazot M, Nassar-Slaba J, Thomassin-Naggara I, Cortez A, Uzan S, Daraï E. MR imaging compared with intraoperative frozen-section examination for the diagnosis of adnexal tumors; correlation with final histology. Eur Radiol. 2006 Dec;16[12]:2687-99. doi: 10.1007/s00330-006-0163-z.
10. Moyle P, Addley HC, Sala E. Radiological staging of ovarian carcinoma. Semin Ultrasound

CT MR. 2010 Oct;31[5]:388-98. doi: 10.1053/j.sult.2010.07.003.

11. Foti PV, Attinà G, Spadola S, Caltabiano R, Farina R, Palmucci S, *et al*. MR imaging of ovarian masses: classification and differential diagnosis. Insights Imaging. 2016 Feb;7[1]:21-41. doi: 10.1007/s13244-015-0455-4.

12. Lam CZ, Chavhan GB. Magnetic resonance imaging of pediatric adnexal masses and mimics. Pediatr Radiol. 2018 Aug;48[9]:1291-1306. doi: 10.1007/s00247-018-4073-4.

13. Sohaib SA, Mills TD, Sahdev A, Webb JA, Vantrappen PO, Jacobs IJ, Reznek RH. The role of magnetic resonance imaging and ultrasound in patients with adnexal masses. Clin Radiol. 2005 Mar;60[3]:340-8. doi: 10.1016/j.crad.2004.09.007.

14. Adusumilli S, Hussain HK, Caoili EM, Weadock WJ, Murray JP, Johnson TD, Chen Q, Desjardins B. MRI of sonographically indeterminate adnexal masses. AJR Am J Roentgenol. 2006 Sep;187[3]:732-40. doi: 10.2214/AJR.05.0905.

15. Messina C, Bignone R, Bruno A, Bruno A, Bruno F, Calandri M, *et al*. Diffusion-Weighted Imaging in Oncology: An Update. Cancers [Basel]. 2020 Jun 8;12[6]:1493. doi: 10.3390/cancers12061493.

16. Bakir B, Bakan S, Tunaci M, Bakir VL, Iyibozkurt AC, Berkman S, Bengisu E, Salmaslioglu A. Diffusion-weighted imaging of solid or predominantly solid gynaecological adnexial masses: is it useful in the differential diagnosis? Br J Radiol. 2011 Jul;84[1003]:600-11. doi: 10.1259/bjr/90706205.

17. Kim HJ, Lee SY, Shin YR, Park CS, Kim K. The Value of Diffusion-Weighted Imaging in the Differential Diagnosis of Ovarian Lesions: A Meta-Analysis. PLoS One. 2016 Feb 23;11[2]:e0149465. doi: 10.1371/journal.pone.0149465.

18. Li W, Chu C, Cui Y, Zhang P, Zhu M. Diffusion-weighted MRI: a useful technique to discriminate benign versus malignant ovarian surface epithelial tumors with solid and cystic components. Abdom Imaging. 2012 Oct;37[5]:897-903. doi: 10.1007/s00261-011-9814-x.

19. Koc Z, Erbay G, Ulusan S, Seydaoglu G, Aka-Bolat F. Optimization of b value in diffusion-weighted MRI for characterization of benign and malignant gynecological lesions. J Magn Reson Imaging. 2012 Mar;35[3]:650-9. doi: 10.1002/jmri.22871.

20. Iorio E, Mezzanzanica D, Alberti P, Spadaro F, Ramoni C, D'Ascenzo S, *et al*. Alterations of choline phospholipid metabolism in ovarian tumor progression. Cancer Res. 2005 Oct 15;65[20]:9369-76. doi: 10.1158/0008-5472.CAN-05-1146.

21. Esseridou A, Di Leo G, Sconfienza LM, Caldiera V, Raspagliesi F, Grijuela B, *et al*. In vivo detection of choline in ovarian tumors using 3D magnetic resonance spectroscopy. Invest Radiol. 2011 Jun;46[6]:377-82. doi: 10.1097/RLI.0b013e31821690ef.

22. Vang R, Shih IeM, Kurman RJ. Ovarian low-grade and high-grade serous carcinoma: pathogenesis, clinicopathologic and molecular biologic features, and diagnostic problems. Adv Anat Pathol. 2009 Sep;16[5]:267-82. doi: 10.1097/PAP.0b013e3181b4fffa.

23. Li WH, Chu CT, Zhang P. MRI and MRS analysis of ovarian endometrioid carcinomas. J Clin Radiol China. 2008;27:470-2

24. El-Sorogy L, Abd-Elgaber N, Omran E, Elshamy M, Youssef H. Role of diffusion MRI and proton magnetic resonance spectroscopy in characterization of ovarian neoplasms. Egyptian J Radiol Nuclear Med. 2012 Mar 1;43[1]:99-106.

25. Forstner R, Meissnitzer MW, Schlattau A, Spencer JA. MRI in ovarian cancer. Imag Med. 2012 Feb 1;4[1]:59-75.

26. Kang YH, Kim MY, Kim KT, Kim YJ, Suh CH, Kim JM, *et al*. H1 Magnetic Resonance Spectroscopy of Cystic Ovarian Lesions. J Korean Soc Magnet Reson Med. 2013 Dec 1;17[4]:326-33.

27. Vargas HA, Barrett T, Sala E. MRI of ovarian masses. J Magn Reson Imaging. 2013 Feb;37[2]:265-81. doi: 10.1002/jmri.23721.

28. Abramov Y, Carmi S, Anteby SO, Ringel I. Ex vivo 1H and 31P magnetic resonance spectroscopy as a means for tumor characterization in ovarian cancer patients. Oncol Rep. 2013 Jan;29[1]:321-8. doi: 10.3892/or.2012.2071.

29. Cho NH, Kim YT, Lee JH, Song C, Cho SW, Cho SH, Chi JG. Diagnostic challenge of fetal ontogeny and its application on the ovarian teratomas. Int J Gynecol Pathol. 2005 Apr;24[2]:173-82. doi: 10.1097/01.rct.0000157093.21809.e7.

30. Takeuchi M, Matsuzaki K, Harada M. Preliminary observations and diagnostic value of lipid peak in ovarian thecomas/fibrothecomas using in vivo proton MR spectroscopy at 3T. J Magn Reson Imaging. 2012 Oct;36[4]:907-11. doi: 10.1002/jmri.23711.

International Journal of Medical Arts

https://ijma.journals.ekb.eg/
Print ISSN: 2636-4174
Online ISSN: 2682-3780